Author Manuscript

Author Manuscript

Author Manuscript

Author Manuscript

HHS Public Access

Author manuscript

Eur J Immunol. Author manuscript; available in PMC 2016 November 01.

Published in final edited form as:

Eur J Immunol. 2015 November ; 45(11): 3073–3086. doi:10.1002/eji.201545569.

Lipocalin-2 ensures host defense against *Salmonella* Typhimurium by controlling macrophage iron homeostasis and immune response

Manfred Nairz[1,*], **Andrea Schroll**[1], **David Haschka**[1], **Stefanie Dichtl**[1], **Thomas Sonnweber**[1], **Igor Theurl**[1], **Milan Theurl**[1], **Ewald Lindner**[1], **Egon Demetz**[1], **Malte Aβhoff**[1], **Rosa Bellmann-Weiler**[1], **Raphael Müller**[1], **Romana R. Gerner**[2], **Alexander R. Moschen**[2], **Nadja Baumgartner**[3], **Patrizia L. Moser**[4], **Heribert Talasz**[5], **Herbert Tilg**[2], **Ferric C. Fang**[6], and **Günter Weiss**[1,*]

[1]Department of Internal Medicine VI, Infectious Diseases, Immunology, Rheumatology, Pneumology, Medical University of Innsbruck, Austria

[2]Department of Internal Medicine I, Gastroenterology, Endocrinology and Metabolism, Medical University of Innsbruck, Austria

[3]Department of Internal Medicine II, Gastroenterology and Hepatology, Medical University of Innsbruck, Austria

[4]Department of Pathology, Medical University of Innsbruck, Austria

[5]Biocenter, Division of Clinical Biochemistry, Medical University of Innsbruck, Austria

[6]Departments of Laboratory Medicine and Microbiology, University of Washington, Seattle, USA

Abstract

Lipocalin-2 (Lcn2) is an innate immune peptide with pleiotropic effects. Lcn2 binds iron-laden bacterial siderophores, chemo-attracts neutrophils and has immunomodulatory and apoptosis-regulating effects.

In this study we show that upon infection with *Salmonella enterica* serovar Typhimurium, Lcn2 promotes iron export from *Salmonella*-infected macrophages, which reduces cellular iron content and enhances the generation of pro-inflammatory cytokines. Lcn2 represses IL-10 production while augmenting Nos2, TNF-α and IL-6 expression. *Lcn2*$^{-/-}$ macrophages have elevated IL-10 levels as a consequence of increased iron content. The crucial role of Lcn-2/IL-10 interactions was further demonstrated by the greater ability of *Lcn2*$^{-/-}$ *IL-10*$^{-/-}$ macrophages and mice to control intracellular *Salmonella* proliferation in comparison to *Lcn2*$^{-/-}$ counterparts. Over-expression of the iron exporter ferroportin-1 in *Lcn2*$^{-/-}$ macrophages represses IL-10 and restores TNF-α and IL-6 production to the levels found in *wild-type* macrophages, so that killing and clearance of intracellular *Salmonella* is promoted.

[*]Correspondence: Guenter Weiss or Manfred Nairz, Medical University, Department of Internal Medicine VI, Infectious Diseases, Immunology, Rheumatology, Pneumology, Anichstr. 35; A-6020 Innsbruck, Austria, Phone: +43-512-504-23251, Fax: +43-512-504-23317, guenter.weiss@i-med.ac.at or manfred.nairz@i-med.ac.at.

Conflict of interest: The authors declare no commercial or financial conflict of interests.

Author Manuscript Author Manuscript Author Manuscript Author Manuscript

Our observations suggest that Lcn2 promotes host resistance to *Salmonella* Typhimurium infection by binding bacterial siderophores and suppressing IL-10 production, and that both functions are linked to its ability to shuttle iron from macrophages.

Keywords

Lipocalin-2; iron; macrophage; IL-10; *Salmonella*

Introduction

Salmonella enterica serovar Typhimurium is a Gram-negative facultative intracellular pathogenic bacterium that replicates within macrophages and requires iron to exert full virulence and to establish infection [1, 2]. To gain sufficient access to iron within the host, *Salmonella* Typhimurium utilizes several acquisition systems. On the one hand, *Salmonella* Typhimurium produces siderophores which capture iron from host proteins due to their extraordinarily high affinity for the metal. In iron-limiting conditions, *Salmonella* synthesizes enterobactin, its prototypical catecholate-type siderophore, by a multi-step process involving EntC (isochorismate synthetase). Following secretion, iron-laden catecholate-type siderophores are bound by receptors on the outer membrane of *Salmonella* [3-6]. On the other hand, non-siderophore bound ferrous iron is taken up by the Feo and Sit systems, respectively [7-10]. Both siderophore-dependent and -independent pathways of iron acquisition are up-regulated upon infection and are linked to *Salmonella* virulence.

While promoting the replication of most viral, bacterial, fungal and protozoan pathogens, iron exerts diverse effects on immune cells thus influencing several aspects of the host-microbe interplay [11-14]. Iron inhibits the production of TNF-α and reactive nitrogen species (RNS) as it inhibits the transcription of NO synthase (Nos)-2 [15]. In contrast, the generation of ROS by Fenton/Haber-Weiss chemistry requires iron as essential cofactor.

The host has evolved numerous strategies to counteract microbial iron acquisition [11, 16]. In the setting of acute infection, the extracellular space is depleted of iron [17, 18], which is retained in cells of the mononuclear phagocyte system (MPS) and sequestered within the iron-storage protein ferritin (Ft) [15, 19-22]. In parallel, the antimicrobial peptide hepcidin-1 (Hamp1) is produced during inflammation [23, 24]. Hamp1 targets ferroportin-1 (Fpn1) and induces its internalization from the cell surface membrane, which subsequently results in Fpn-1 degradation and reduction of cellular iron efflux [25]. As a consequence, duodenal iron absorption and iron recycling from the MPS are hampered, which reduces serum iron levels. This mechanism is thought to be beneficial in the presence of extracellular bacteria by limiting their excess to the nutrient iron [15, 16, 26, 27]. Upon infection of macrophages with intracellular microbes, however, Hamp1-induced Fpn1-internalization is counter-productive as this mechanism increases the intracellular iron content and facilitates iron access for pathogens within infected cells [28]. Consequently, inhibition of Hamp1 formation improves host defense against *Salmonella* [29]. Nos2 mediates the induction of Fpn1 transcription in macrophages infected with *Salmonella* Typhimurium, thus counter-balancing Hamp1 function [30].

Author Manuscript Author Manuscript Author Manuscript Author Manuscript

Further, the multi-functional protein lipocalin-2 (Lcn2) is released by monocytic cells to limit the availability of iron for invading microbes. In its primary role, Lcn2 captures bacterial siderophores including enterobactin produced by *Salmonella* Typhimurium and other enterobacteriaceae such as *Escherichia coli* and *Klebsiella pneumoniae* [31-33] as well as carboxymycobactins generated by mycobacteria [34-36].

Second, Lcn2 affects mammalian iron homeostasis by siderophore-dependent processes. Lcn2 binds iron-laden siderophores, thus mediating iron uptake via Lcn2 receptor (LcnR). On the other hand, iron-free siderophores can be imported through LcnR-mediated endocytosis. Intracellularly, these apo-siderophores bind iron for subsequent LcnR-dependent export. In cells over-expressing LcnR, this mechanism causes iron depletion and induces apoptosis [37]. In addition, mammalian siderophores have been identified [38, 39], which may fulfill central functions in mammalian iron homeostasis including the regulation of cytoplasmic iron levels [40].

Third, Lcn2 promotes the production of the chemokine IL-8 and, independently, stimulates the chemotaxis of neutrophils by an ERK1/2-mediated mechanism [41, 42].

While the role of Lcn2 in neutrophils and in *Salmonella* enterocolitis is well established [42-44], little is known about its function in macrophages and in the course of *Salmonella* septicemia. We therefore systematically investigated the role of Lcn2 in the setting of *Salmonella* Typhimurium infection and observed that Lcn2 production has distinct effects on macrophage iron homeostasis and immune response.

Lcn2$^{-/-}$ mice infected with *Salmonella* had higher bacterial burdens in spleen and liver due to a shift of the immune response towards an anti-inflammatory phenotype characterized by increased IL-10 levels and reduced expression of Nos2, TNF-α and IL-6. Furthermore, *Lcn2*$^{-/-}$ macrophages had increased cellular iron content and produced higher amounts of IL-10, which could be reversed by the iron chelator deferasirox (DFX) or upon over-expression of the iron exporter FPN1. Increased IL-10 production played a central role in the immune dysfunction of *Lcn2*$^{-/-}$ macrophages as its neutralization restored the generation of NO and TNF-α. The high IL-10 production contributed to the poor control of *Salmonella* by *Lcn2*$^{-/-}$ macrophages, as *Lcn2*$^{-/-}$ *IL10*$^{-/-}$ macrophages killed *Salmonella* substantially better than IL-10-producing *Lcn2*$^{-/-}$ cells.

The findings presented herein expand our knowledge on the pleiotropic immune-regulatory effects of Lcn2. Lcn2 limits macrophage iron content and IL-10 production thus ensuring efficient host defense against *Salmonella* Typhimurium. Therefore, Lcn2 links the maintenance of macrophage iron homeostasis to their antibacterial effector functions.

Results

Lcn2 regulates macrophage iron content upon *Salmonella* Typhimurium infection

Upon infection of thioglycolate-elicited peritoneal macrophages with *Salmonella* Typhimurium, we observed a time-dependent massive increase of Lcn2 mRNA levels (Fig. 1A). The induction of Lcn2 mRNA became highly significant as early as 1.5 h after

Author Manuscript Author Manuscript Author Manuscript Author Manuscript

Salmonella infection and peaked after 18 h. To study a potential influence of Lcn2 on macrophage iron homeostasis, we isolated thioglycolate-elicited peritoneal macrophages from *Lcn2*$^{-/-}$ mice on a C57BL/6 background and from *Lcn2*$^{+/+}$ littermates. At 24 h after infection with *Salmonella* Typhimurium (*S*. Tm.), primary *Lcn2*$^{-/-}$ macrophages had increased iron contents as compared to their *wild-type* (*wt*) counterparts (Fig. 1B). This was attributable to impaired iron export from *Lcn2*$^{-/-}$ macrophages (Fig. 1C), while iron import was not different between *Lcn2*$^{-/-}$ and *Lcn2*$^{+/+}$ macrophages (data not shown). In line, the number of intracellular *Salmonella* was significantly higher in *Lcn2*$^{-/-}$ than in *Lcn2*$^{+/+}$ macrophages after 24 h (Fig. 1D), whereas no difference was observed in *Salmonella* uptake by macrophages after 30 min (Fig.1E).

Increased IL-10 mRNA expression in *Lcn2*$^{-/-}$ macrophages

Given the higher iron content of *Lcn2*$^{-/-}$ peritoneal macrophages and the known influence of iron on macrophage functions, we tested the regulation of immune response genes as a function of Lcn2 expression over time. Following infection with *Salmonella* Typhimurium, we observed that as early as 3 h after the initiation of infection, *Lcn2*$^{-/-}$ macrophages (open symbols) expressed higher IL-10 mRNA levels as compared to their *wt* counterparts (Fig. 2A, closed symbols). In contrast, TNF-α mRNA expression was significantly lower in infected macrophages from *Lcn2*$^{-/-}$ than from *wt* mice over time, which was also true of IL-6 and Nos2 expression at several but not all time points investigated (Fig. 2B, C and D). The increased IL-10 mRNA levels observed in *Lcn2*$^{-/-}$ macrophages translated into increased IL-10 concentrations in culture supernatants of *Salmonella*-infected *Lcn2*$^{-/-}$ macrophages (Fig. 2E).

The enhanced production of IL-10 in *Lcn2*$^{-/-}$ macrophages appeared to be independent from TNF-α expression as the neutralization of TNF-α with a specific antibody did not alter the differences in bacterial killing or IL-10 secretion between peritoneal macrophages isolated from *Lcn2*$^{-/-}$ or *wt* mice (Supporting Information Fig. 1A and B). The accumulation of nitrite in culture supernatants, which was significantly dependent on the *Lcn2* genotype in cells treated with the isotype control antibody, was reduced by the TNF-α antibody in both *Lcn2*$^{-/-}$ and *wt* macrophages (Supporting Information Fig. 1C). Notably, exposure of macrophages to the same number of heat-inactivated *Salmonella* did not cause substantial differences in IL-10 mRNA expression between cells of the two genotypes (Fig. 2F). The influence of Lcn2 deficiency on macrophage IL-10 expression was not secondary to an increased bacterial load, as infection of macrophages with *entC sit feo* or *aro* mutant *Salmonella*, which are compromised in replication due to targeted defects in iron uptake or synthesis of aromatic amino acids, respectively, also resulted in a significant difference in IL-10 mRNA production (data not shown).

Furthermore, the effect was independent of the presence of other bacterial pathogenicity genes such as *invA*, *Salmonella pathogenicity island (SPI)-1*, *SPI-2* or *phoP*, as infection of *wt* and *Lcn2*$^{-/-}$ macrophages with *Salmonella* strains deficient in these genes did not abolish the differences in IL-10 mRNA expression (data not shown). This was also true for infection with *Salmonella* carrying a mutation of lipid A (*waaN* mutant) or flagellin (*fliC fljB* mutant)

Author Manuscript Author Manuscript Author Manuscript Author Manuscript

biosynthesis, which results in reduced stimulation of TLR4 and TLR5, respectively (Fig. 3A).

In contrast, stimulation with TLR ligands MALP-2, PAM2Cys, PAM3Cys, Poly:ICs, LPS and flagellin did not result in significantly different IL-10 mRNA or protein expression between macrophages of the two genotypes (Fig. 3A and 3B and data not shown). Interestingly, infection with the intracellular pathogens *Chlamydia pneumoniae* or *Listeria monocytogenes* also resulted in increased IL-10 mRNA and protein expression by *Lcn2*$^{-/-}$ macrophages, whereas challenging of macrophages with the extracellular bacteria *E. coli* or *Klebsiella pneumoniae* did not cause differences in IL-10 mRNA expression between *wt* and *Lcn2*$^{-/-}$ macrophages. Exposure of macrophages to *Staphylococcus aureus* resulted in reduced IL-10 mRNA and protein levels in *Lcn2*$^{-/-}$ as compared to *wt* macrophages (Fig. 3C and 3D).

Exposure to *Salmonella* Typhimurium resulted in differential IL-10 expression between *wt* and *Lcn2*$^{-/-}$ macrophages. However, the addition of cytochalasin D (CytD) which inhibits the internalization of bacteria (and was effective as determined by selective plating) as well as actin cytoskeletal rearrangements did not affect this differential IL-10 production (Fig. 3E and data not shown).

As Lcn2 has been implicated in the control of apoptosis, we performed additional *in vitro* experiments to look for differences in cell death between *Salmonella*-infected *wt* and *Lcn2*$^{-/-}$ macrophages. However, we did not see significant differences in annexin V or propidium iodide staining, or caspase-1 activation (Supporting InformationFig. 2A, B and C). Furthermore, IL-1β secretion, another indicator of caspase-1 activity, was not different between *wt* and *Lcn2*$^{-/-}$ macrophages (data not shown).

Low intracellular iron suppresses IL-10 and restores effector functions in *Lcn2*$^{-/-}$ macrophages

In view of the increased iron content of *Lcn2*$^{-/-}$ peritoneal macrophages, we tried to rescue the phenotype of *Lcn2*$^{-/-}$ cells by forced expression of the iron exporter FPN1 in macrophages. We saw that transfection of *wt* (Fig. 4A, closed bars) and *Lcn2*$^{-/-}$ macrophages (Fig. 4A, open bars) with WT FPN1 and the FPN1 N144H variant (conferring partial resistance to Hamp1) significantly increased iron release from both cells and abrogated the differences observed between these two genotypes, both at steady state conditions and after infection with *Salmonella*. In contrast, expression of the FPN1 A77D mutant, which is retained in the cytoplasm, was without any effect. Furthermore, the differences in bacterial load and IL-10 secretion between *wt* and *Lcn2*$^{-/-}$ peritoneal macrophages were specifically abrogated by over-expression of WT FPN1 and the FPN1 N144H variant in these macrophages (Fig. 4B and C). In contrast, over-expression of the FPNA77D variant, which is unable to mount transcellular iron export due to its intracellular retention, had no effect. Similarly, treatment of infected macrophages with the iron chelator DFX significantly reduced IL-10 secretion and bacterial loads in *wt* and *Lcn2*$^{-/-}$ macrophages and abrogated the differences between the two genotypes (Fig. 4D and E).

Author Manuscript Author Manuscript Author Manuscript Author Manuscript

To confirm that the increased expression of Fpn1 is related to improved control of infection with *Salmonella*, we used constructs coding for FPN1-EmGPF fusion proteins to rescue *Lcn2*$^{-/-}$ peritoneal macrophages (Fig. 5). At a transfection rate of 71 ± 5% we were able to assess the intracellular bacterial load in GFP^{+} cells over-expressing FPN1 and compare it to the bacterial load observed in un-transfected GFP^{-} macrophages not over-expressing FPN1 (Fig. 5B, D and F). Over-expression of FPN1 resulted in improved control of infection in GFP^{+} macrophages (Fig. 5B) as reflected by low or no bacterial counts in these cells whereas GFP^{-} macrophages harbored more bacteria after 16 h of infection (see Fig. 5B and compare GFP^{+} and GFP^{-} cells in Fig. 5D and F). In addition, the over-expression of FPN1 in GFP^{+} *Lcn2*$^{-/-}$ cells rescued their phenotype (Fig. 5B and F), whereas transfection with a control plasmid encoding EmGFP but not FPN1 did not show this effect (Fig. 5A and E).

Targeting IL-10 rescues the phenotype of *Lcn2*$^{-/-}$ macrophages and mice

To study the functional consequence of differential expression of the anti-inflammatory mediator IL-10 between *wt* and *Lcn2*$^{-/-}$ macrophages, we infected cells in the presence and absence of neutralizing antibody against IL-10 or CD-210, a subunit of the IL-10 receptor. Either antibody abrogated the differences in bacterial load (Fig. 6A) and NO output (Fig. 6B) between *wt* and *Lcn2*$^{-/-}$ macrophages. While antibody-mediated blockade of IL-10 signaling promoted TNF-α generation in both *wt* and *Lcn2*$^{-/-}$ macrophages (Fig. 6C), the differences between cells of the two genotypes were not fully eliminated. Importantly, we found that *Lcn2*$^{-/-}$ *IL-10*$^{-/-}$ thioglycolate-elicited peritoneal macrophages controlled *Salmonella* Typhimurium significantly better than *Lcn2*$^{-/-}$ (i.e., *Lcn2*$^{-/-}$ *IL-10*$^{+/+}$) cells (Fig. 6D). Similar effects of Lcn2 on bacterial loads and IL-10 production were observed in non-elicited previously naïve peritoneal macrophages. Moreover, bacterial loads in infected BMDM from *Lcn2*$^{-/-}$ *IL-10*$^{-/-}$ mice were comparable to that from *IL-10*$^{-/-}$ mice (Supporting Information Fig. 3A-3D).

We then looked for differences in the immune response between *wt* and *Lcn2*$^{-/-}$ mice upon systemic *Salmonella* Typhimurium infection. Of note, *Lcn2*$^{-/-}$ mice infected with *Salmonella* harbored significantly more bacteria in spleen and liver (Fig. 7A and data not shown) and had increased IL-10 mRNA levels in the spleen as compared to *wt* mice (Table 1). This translated into increased IL-10 serum concentrations (Fig. 7B). In contrast, mRNA levels of Nos2, TNF-α and IL-6 were substantially reduced in the spleen of *Salmonella*-infected *Lcn2*$^{-/-}$ mice (Table 1). Correspondingly, serum TNF-α and IL-6 concentrations were lower in *Lcn2*$^{-/-}$ mice (Fig. 7C and 7D).

Importantly, treatment with a neutralizing monoclonal IL-10 antibody (α IL-10; depicted as grey circles in Fig. 7E) could to a large degree rescue the phenotype of *Lcn2*$^{-/-}$ mice (open circles) resulting in significantly lower splenic bacterial loads than observed in *Lcn2*$^{-/-}$ mice treated with solvent (PBS) or a non-neutralizing IgG control antibody (isotype). There was no difference in the bacterial load in the spleen of solvent-treated *wt* mice (closed circles) as compared to α IL-10 treated *Lcn2*$^{-/-}$ mice (Fig. 7E). Furthermore, in the spleen, the bacterial load in *Lcn2*$^{-/-}$ *IL-10*$^{-/-}$ mice (grey circles) was significantly lower than in *Lcn2*$^{-/-}$ mice (open circles) and not different from *wt* mice (Fig. 7F, closed circles). This difference was

Author Manuscript Author Manuscript Author Manuscript Author Manuscript

paralleled by increased TNF- α and IL-6 serum levels in *Lcn2*$^{-/-}$ *IL-10*$^{-/-}$ mice as compared to *Lcn2*$^{-/-}$ mice (Supporting Information Fig. 4A and 4B).

In addition, mice were infected with *wt Salmonella* Typhimurium or an isogenic *entC* mutant unable to produce any catecholate-type siderophores. The bacterial load in liver (not shown) and spleen (Fig. 7G) was lower in *wt* (closed symbols) than in *Lcn2*$^{-/-}$ mice (open symbols) 72 h after bacterial injection, independent of the capacity of *Salmonella* to produce catecholate-type siderophores. Thus, in the absence of siderophore production by *Salmonella*, *Lcn2*$^{-/-}$ mice continued to display higher bacterial load than *wt* mice (Fig. 7G) paralleled by increased serum IL-10 levels (data not shown).

Discussion

In being an essential cofactor for numerous processes in both mammalian and microbial metabolism, iron plays a central role in host-pathogen interactions [12, 14, 45]. In the classical view, the immune response in the course of a bacterial infection directs iron fluxes into the MPS and results in the safe sequestration of iron within Ft [11, 15, 16]. This diversion of iron trafficking renders iron unavailable for extracellular pathogens and is driven by pro-inflammatory cytokines that stimulate iron uptake and Ft expression, and by Hamp1, which stops Fpn1-mediated iron export [25, 29].

Lcn2 has initially been described as a granule-derived secretion product of neutrophils [46, 47]. However, little is known about the interactions of neutrophils and iron homeostasis under either steady state conditions or during infections. Lcn2 is generated by a range of cell types including macrophages. We therefore studied the regulation of iron metabolism upon infection with a facultative intracellular bacterium, *Salmonella* Typhimurium, which invades monocytes and macrophages in order to spread systemically within MPS organs of the host [1]. We report that the antimicrobial peptide Lcn2 exerts essential regulatory functions in macrophage iron homeostasis and is required for an efficient pro-inflammatory immune response in the setting of *Salmonella* Typhimurium infection. The induction of Lcn2 synthesis following *Salmonella* infection was required to limit the macrophage iron content upon *Salmonella* infection. Furthermore, *Lcn2*$^{-/-}$ mice and macrophages were characterized by a shift of the immune response to an anti-inflammatory phenotype dominated by increased production of IL-10. The increased IL-10 expression of *Lcn2*$^{-/-}$ macrophages was a consequence of intracellular iron accumulation in these cells and could be reversed by the addition of the iron chelator DFX or by forced expression of functional FPN1 variants. In contrast, blockade or supplementation of TNF-α could not alter the differences in IL-10 production between *wt* and *Lcn2*$^{-/-}$ macrophages. Furthermore, the enhanced generation of IL-10 by *Lcn2*$^{-/-}$ macrophages was relevant for the outcome of *Salmonella* infection, as antibody-mediated neutralization of IL-10 or blockade of its specific receptor subunit CD-210 resulted in improved control of bacterial replication and restored the production of NO to levels observed in *wt* macrophages. The differences in TNF-α production between *wt* and *Lcn2*$^{-/-}$ cells could not be completely abolished by IL-10 blockade, suggesting the involvement of additional signaling events. Time-course experiments conducted with both viable and heat-inactivated *Salmonella* support the idea that increased IL-10 expression by *Lcn2*$^{-/-}$ macrophages is an early feature of the dysregulation of the immune response in these

Author Manuscript Author Manuscript Author Manuscript Author Manuscript

cells, while reduced Nos2 expression is the consequence. Thus, by repressing IL-10 production, Lcn2 may amplify the antimicrobial defense against *Salmonella* Typhimurium. Similar results were seen upon infection with the intracellular bacteria *Chlamydia pneumoniae* [48] or *Listeria monocytogenes* (Fig. 3 of this study).

Following infection with *Streptococcus pneumoniae*, Lcn2 has been identified as marker of deactivated macrophages, and *Lcn2*$^{-/-}$ BMDM generated reduced IL-10 mRNA levels [49]. This goes along with our observation that IL-10 production was reduced upon challenge of *Lcn2*$^{-/-}$ macrophages with the Gram-positive bacterium *Staphylococcus aureus*.

Cytochalasin D, an inhibitor of actin polymerization known to interfere with phagocytosis and cytoskeletal rearrangements, resulted in a dose-dependent increase in IL-10 secretion by *Salmonella*-exposed macrophages without affecting the relative differences observed between *wt* and *Lcn2*$^{-/-}$ macrophages. Given that infection of macrophages with *E. coli* or *Klebsiella pneumoniae*, both of which are enterobactin-producing (Gram-negative) enterobacteriaceae with a predominantely extracellular life cycle, did not result in differential IL-10 secretion by *wt* and *Lcn2*$^{-/-}$ macrophages, this result is somewhat unexpected (Fig. 3). Furthermore, we did not observe differences in IL-10 mRNA levels between *wt* and *Lcn2*$^{-/-}$ macrophages or spleens under non-inflammatory conditions (Table and details not shown). This implies that the basal transcription rate of the IL-10 gene in steady-state is not influenced by Lcn2 whose levels are readily detectable in the culture supernatant or serum in that situation though (details not shown). However, the presence of extracellular *Salmonella* may stimulate IL-10 secretion by a yet unknown mechanism that is counter-regulated by Lcn2 resulting in increased IL-10 production by *Lcn2*$^{-/-}$ macrophages (Fig. 3). Furthermore, the professional intracellular pathogens *Chlamydia pneumoniae* and *Listeria monocytogenes* (along with intracellular *Salmonella* Typhimurium) may stimulate IL-10 secretion by host macrophages when Lcn2 is absent. This suggests that the signaling pathway responsive to these unrelated intracellular bacteria is influenced by either Lcn2 itself or - indirectly - by intracellular iron which is higher in *Lcn2*$^{-/-}$ macrophages (Fig. 1). The idea that the mechanism is iron-dependent is supported by the results obtained with macrophages overexpressing functional FPN1 or being iron-depleted upon DFX treatment (Fig. 4). The dose-response effect of cytochalasin D on IL-10 secretion by both *wt* and *Lcn2*$^{-/-}$ macrophages further suggests that extracellular *Salmonella* carries a membrane component or produces a soluble mediator that stimulates IL-10 expression in a Lcn2-independent fashion or that signaling processes induced by extracellular *Salmonella* impact on IL-10 expression in that setting. However, based on the data obtained with purified LPS or flagellin, respectively (Fig. 3), and with *Salmonella* mutants this mechanism appears to be independent from classical TLR4- and TLR5 inducible signaling cascades. Additionally, we have ruled out the *Salmonella* pathogenicity island (SPI)-2 and phoP/phoQ systems are involved in this macrophage response using specific *Salmonella* mutants (data not shown). Therefore, it is likely that other PAMPs and PRRs mediate the increased IL-10 expression observed in *Lcn2*$^{-/-}$ macrophages in the setting of *Salmonella* infection.

Alternatively, an actin-dependent endocytotic mechanism preferentially involved in the response to intracellular pathogens may inhibit IL-10 secretion by infected macrophages because blockade of endosomal trafficking is associated with impaired control of *Salmonella*

Author Manuscript Author Manuscript Author Manuscript Author Manuscript

replication within macrophages [50]. Either way, further studies will be required to precisely define the signaling pathways that link Lcn2 to IL-10 transcription in macrophages confronted with intracellular bacteria.

A growing number of reports demonstrate that Lcn2 is important in the control of pathogens that do not produce siderophores or whose siderophores cannot be captured by Lcn2 [48]. These pathogens controlled by Lcn2 by siderophore-independent mechanisms include *Chlamydia pneumoniae*, *Staphylococcus aureus* and *Candida albicans*. Moreover, differences in serum iron levels between *wt* and *Lcn2*$^{-/-}$ mice following challenge with pure LPS have been reported [51]. We observed that there is a significant difference in the number of *entC* mutant *Salmonella* Typhimurium in liver and spleen of *wt* as compared to *Lcn2*$^{-/-}$ mice. This is of interest as the *entC* mutant is unable to synthesize the Lcn2 target enterobactin. These results thus imply a dual mechanism by which Lcn2 combats infection with *Salmonella* Typhimurium. One mechanism is the interference of Lcn2 with enterobactin-mediated bacterial iron acquisition. The importance of this host iron restriction strategy is evident from the comparison of the bacterial load of *wt* vs. *entC* mutant *Salmonella* Typhimurium. Second, there is a Lcn2-mediated antibacterial mechanism that is independent of its ability to bind bacterial siderophores. Our data obtained with antibody-mediated neutralization of circulating IL-10 and with *Lcn2*$^{-/-}$ *IL-10*$^{-/-}$ mice suggest that this mechanism is mediated via IL-10. We therefore conclude that in the course of infection with Gram-negative bacteria, Lcn2 also functions as a negative regulator of IL-10 by mediating cellular iron export. Lcn2 thus links the maintenance of iron homeostasis in macrophages to an efficient pro-inflammatory and antimicrobial immune response, which is of pivotal importance in host resistance to *Salmonella* Typhimurium infection.

Materials and Methods

Cell isolation and culture

C57BL/6N type mice (*wt*, *Lcn2*$^{+/+}$), congenic *Lcn2*$^{-/-}$ mice [31], *IL-10*$^{-/-}$ mice and *Lcn2*$^{-/-}$*IL-10*$^{-/-}$ mice, backcrossed onto a C57BL/6N background for at least 12 generations, were used in these studies. To generate *Lcn2*$^{-/-}$*IL-10*$^{-/-}$ mice, *IL-10*$^{-/-}$ mice [57] were obtained (The Jackson Laboratory) and intercrossed with *Lcn2*$^{-/-}$ mice. Following genotyping, littermates were housed in neighbouring cages under specific pathogen-free conditions at the central animal facility of the Medical University of Innsbruck.

Thioglycolate-elicited or non-elicited naïve peritoneal macrophages were harvested from *Lcn2*$^{+/+}$ C57BL/6N and congenic *Lcn2*$^{-/-}$ mice, *IL-10*$^{-/-}$ mice or *Lcn2*$^{-/-}$*IL-10*$^{-/-}$ mice, respectively, and cultured as detailed elsewhere [30]. BMDM were harvested from tibiae and femora and cultured for 7 days in the presence of 50 ng/ml recombinant murine M-CSF (Preprotech). Macrophages were incubated in RPMI and stimulated with phosphate buffered saline (PBS; Lonza), 100 ng/ml LPS (lipopolysaccharide from *Salmonella* Typhimurium used as a TLR4 ligand; Sigma-Aldrich), 1 μg/ml MALP-2 (macrophage-activating lipopeptide from *Mycoplasma fermentans* used as a TLR2/6 ligand; Alexis), 100 ng/ml Pam_2Cys (TLR2/6 ligand; EMC microcollections), 100 ng/ml Pam_3Cys (used as TLR1/2 ligand; purchased from EMC microcollections), 10 μg/ml Poly(I:C) (TLR3 ligand; Sigma-Aldrich) or 100 ng/ml flagellin (from *Salmonella* Typhimurium; TLR5 ligand; Enzo) .

Author Manuscript Author Manuscript Author Manuscript Author Manuscript

The purity of the resulting cell suspension was tested by fluorescent-activated cell sorting analysis and exceeded 95% [58]. Intracellular iron concentrations in macrophages were determined by atomic absorption as described [58].

For macrophage iron export assays, cells were treated and infected with *S.* Typhimurium as detailed above and iron export determined with 5 μM ^{59}Fe-citrate exactly as previously described [30]. In parallel to each iron release study, a trypan-blue exclusion assay was performed to ensure that neither treatment interfered with macrophage integrity and viability.

Salmonella infection in vitro

Prior to *in vitro* infection, macrophages were extensively washed with PBS and incubated in complete RPMI without antibiotics. Unless otherwise indicated, *wt Salmonella enterica* serovar Typhimurium (*S.* Typhimurium) strain ATCC14028 was used for experiments and grown under sterile conditions in LB broth (Sigma-Aldrich) to late-logarithmic phase. Macrophages were infected with *S.* Typhimurium at a multiplicity of infection (MOI) of 10 for 1 h. Thereafter, cells were washed with PBS and incubated in complete RPMI containing gentamicin (Gibco). Where appropriate, cells were subsequently treated with 50 μM deferasirox (DFX; Novartis), a monoclonal rat anti-mouse IL-10 antibody (10 μg/ml; clone JES5-2A5), a monoclonal rat anti-mouse CD-210 antibody (10 μg/ml; clone 1B1.3a), a monoclonal rat anti-mouse TNF-α antibody (10 μg/ml; clone MP6-XT22), or the appropriate isotype controls (10 μg/ml; all from Biolegend) for up to 23 h. Where appropriate, cells were preincubated in 0.1 to 50 μg/ml cytochalasin D (CytD; Sigma-Aldrich) 1 hr prior to the infection.

To determine intracellular bacterial loads, infected cells were harvested in 0.5% sodium deoxycholic acid (Sigma-Aldrich) as described [52]. To determine bacterial uptake, infected cells were harvested after 30 min.

Isogenic *S.* Typhimurium mutants used included *entC*(x02237)*aph*, *entC*:*aph sit*(x02237)*bla feo*(x02237)Tn*10* (Tet), *fepA*(x02237)FRT*cat*FRT, *iroN*(x02237)FRT*kan*FRT, *invA*(x02237)*aph*, *SPI-1*(x02237)*aph*, *SPI-2*(x02237)*kan*, *rpoE*(x02237)*cat*, *phoP102*(x02237)Tn*10dCm*, *aroA*(x02237)Tn*10*, *waaN*(x02237)FRT*kan*FRT and *fliC*(x02237)*cat fljB*(x02237)Tn*10* [1, 3, 52].

Where indicated, *Escherichia coli* (ATCC 25922), *Klebsiella pneumoniae* (ATCC 43816), *Listeria monocytogenes* EGDe (ATCC BAA-679; kindly provided by Thomas Decker, Max F. Perutz Laboratories, Department of Genetics, Microbiology and Immunobiology, University of Vienna, Austria) or *Staphylococcus aureus* (ATCC 11632) were used for *in vitro* infections at a MOI of 10:1. The *Chlamydia pneumoniae* strain CV-6 (kindly provided by Jan Rupp, Institute of Medical Microbiology and Hygiene, University of Lübeck, Germany) was cultivated and propagated as described earlier, and infections were performed at a MOI of 10:1 [53].

Author Manuscript Author Manuscript Author Manuscript Author Manuscript

Plasmids and transient transfection

Human FPN1 and the N144H (conferring partial resistance to Hamp1) and A77D FPN1 (resulting in reduced cell surface expression) mutants, respectively, were cloned into the p-cDNA3.1 expression vector as described elsewhere and kindly provided by Mrs. Lisa Schimanski and Dr. Hal Drakesmith, Weatherall Institute of Molecular Medicine, Oxford, United Kingdom [59]. Transient transfections of primary peritoneal macrophages were performed by means of lipofection using Lipofectamine (Promega).

For immunocytochemistry, we used EmGFP N- or C-terminally tagged human FPN1 expression clones, kindly provided by Dr. Heinz Zoller, Department of Internal Medicine II, Medical University of Innsbruck, Austria [60]. The FPN1 open reading sequence was transferred into Vivid Colors pcDNA 6.2/EmGFP-DEST vectors to create EmGFP FPN1 expression clones. As control vectors, we used Vivid Colors pcDNA 6.2 EmGFP/CAT (chloramphenicol acetyltransferase) plasmids. Efficiency of transfections was at least 71±5%. The use of EmGFP-FPN1 fusion constructs thus allows the determination of the bacterial load at the single-cell level and the direct comparison of cells overexpressing FPN1 (transfected and thus GFP^+) and cells not overexpressing FPN1 (un-transfected and thus GFP^-). Thus, the intracellular *Salmonella* load can be analyzed as a function of FPN1 expression.

peritoneal macrophages were seeded on glass slides, transfected and subsequently infected for 16-24 h as described [30]. Cells were incubated with antibodies as follows: a chicken GFP antibody (1:1000; Invitrogen), a goat CSA1 (for *Salmonella* common structural antigen) antibody (1:1,000; KPL) and appropriate fluorochrome-conjugated secondary antibodies, i.e., rabbit anti-chicken Alexa Fluor 488 (green; 1:1,000; Dianova) and donkey anti-goat Alexa 594 (red; 1:1,000; Invitrogen). In independent experiments, cells were stained with annexin V (BioLegend) or propidium iodide (Sigma) according to the manufacturer's recommendations. For microscopic analysis, cells were covered with Fluorescent Mounting Medium (DAKO) containing DAPI and analyzed under an Axioskop 2 microscope (Carl Zeiss). Acquisition was done using the Carl Zeiss AxioCam MRc 5 camera, a 100×/1.25 objective and AxioVision imaging software version 4.0.

Salmonella infection in vivo

All animal experiments were performed according to the guidelines of the Medical University of Innsbruck based on the Austrian Animal Testing Act of 1988. All animal experiment protocols were approved by the ‘MUI Animal ethics committee’ and the Austrian Ministry for Science and Education (approvals no. BMWF-66.011/0072-II/3b/2012 and no. BMWF-66.011/0142-WF/V/3b/2014). Unless otherwise indicated, male mice were used at 12-16 weeks of age and infected i.p. with 500 CFU of *S.* Typhimurium diluted in 200 µl PBS. Unless otherwise specified, *S.* Typhimurium *wt* strain ATCC 14028s was used for experiments. In some experiments, its isogenic mutant derivative *entC*(x02237)aph was used. This mutant strain was constructed and grown as described [3] and used as detailed above. The bacterial load of organs was determined by plating serial dilutions of organ homogenates on LB agar (Sigma-Aldrich) under sterile conditions and the number of bacteria calculated per gram of tissue.

Author Manuscript Author Manuscript Author Manuscript Author Manuscript

Where appropriate, mice were infected as above and injected i.p. 200 μg of the neutralizing monoclonal anti-mouse IL-10 antibody (clone JES5-2A5) dissolved in 200 μl PBS or the identical amount of an isotype control antibody (all obtained from Biolegend) on d 1 and 2 after infection. Mice were then sacrificed on d 3 of infection.

The determination of tissue iron content was carried out in a 96-well plate following acid hydrolysis at 65°C for 24 h and using a colorimetric solution containing sodium acetate, bathophenanthroline disulfonic acid and L-ascorbic acid. The calculated iron quantity was normalized to the wet tissue weight for each sample. Plasma iron concentration was quantified using a commercially available iron kit (QuantiChrom Iron Assay Kit; BioAssay Systems), exactly following the manufacturer's instructions. Monocyte and neutrophils counts were hemocytometrically quantified using a veterinary animal blood counter (Lab Technologies).

RNA extraction and quantitative real-time PCR

Total RNA was prepared and mRNA expression quantified by quantitative RT-PCR following reverse transcription exactly as described [52]. Hypoxanthine phosphoribosyltransferase (Hprt), β-glucuronidase, β-actin and 18s ribosomal RNA were used as housekeeping genes with similar results [54, 55]. Data are depicted and were analyzed using Hprt as reference gene.

Western blot analysis

Protein extraction and Western blotting were performed using a rat Lcn2 antibody (1:400; R&D), a rabbit Fpn1 antibody (1:400; Eurogentec), a rabbit actin antibody (1:1,000; Sigma-Aldrich) and appropriate HRP-conjugated secondary antibodies (1:1000; Dako).

Detection of cytokines and reactive species

Determination of cytokines in culture supernatants was performed with ELISA kits for TNF-α, IL-6 and IL-10 (BD Pharmingen). Determination of nitrite, the stable oxidation product of nitric oxide (NO), was carried out with the Griess-Ilosvay's nitrite reagent (Merck) as described [52].

Statistical analysis

Statistical analysis was carried out using a SPSS statistical package. We determined significance by unpaired two-tailed *t* test to assess data, when only two groups were compared. For multiple comparisons Analysis of variance (ANOVA) combined with Bonferroni correction was performed. Unless otherwise specified, data are depicted as lower quartile, median and upper quartile (boxes), and minimum/maximum ranges. When Gaussian distribution was not assumed, data were log-transformed prior to *t* test or ANOVA. Generally, *P* values less than 0.05 were considered significant in any test.

Supplementary Material

Refer to Web version on PubMed Central for supplementary material.

Author Manuscript Author Manuscript Author Manuscript Author Manuscript

Acknowledgments

The authors are grateful to Sylvia Berger, Alexandra Bichler, Ines Brosch, Sabine Engl and Markus Seifert for excellent technical support.

The authors thank Dr. Shizuo Akira, Laboratory of Host Defense, Osaka University for providing *Lcn2*$^{-/-}$ mice [31].

The authors are indebted to Mrs. Lisa Schimanski and Drs. Thomas Decker, Hal Drakesmith, Jan Rupp and Heinz Zoller for providing bacteria and plasmids, respectively [53, 56].

This work was supported by grants from the Austrian Research Fund (FWF; project TRP-188 to G.W.), the 'Theodor Körner Fonds' (to M.N.), the intramural funding program of the Medical University Innsbruck for young scientists MUI-START (project 2012032003 to M.N.) and by the 'Verein zur Förderung von Forschung und Weiterbildung in Infektiologie und Immunologie an der Medizinischen Universität Innsbruck'. F.F. is supported by the National Institutes of Health (AI39557 and AI44486).

References

1. Vazquez-Torres A, Jones-Carson J, Baumler AJ, Falkow S, Valdivia R, Brown W, Le M, et al. Extraintestinal dissemination of Salmonella by CD18-expressing phagocytes. Nature. 1999; 401:804–808. [PubMed: 10548107]
2. Collins HL. The role of iron in infections with intracellular bacteria. Immunol Lett. 2003; 85:193–195. [PubMed: 12527227]
3. Crouch ML, Castor M, Karlinsey JE, Kalhorn T, Fang FC. Biosynthesis and IroC-dependent export of the siderophore salmochelin are essential for virulence of Salmonella enterica serovar Typhimurium. Mol Microbiol. 2008; 67:971–983. [PubMed: 18194158]
4. Nagy TA, Moreland SM, Andrews-Polymenis H, Detweiler CS. The Ferric Enterobactin Transporter Fep Is Required for Persistent Salmonella enterica Serovar Typhimurium Infection. Infect Immun. 2013; 81:4063–4070. [PubMed: 23959718]
5. Hantke K, Nicholson G, Rabsch W, Winkelmann G. Salmochelins, siderophores of Salmonella enterica and uropathogenic Escherichia coli strains, are recognized by the outer membrane receptor IroN. Proc Natl Acad Sci U S A. 2003; 100:3677–3682. [PubMed: 12655053]
6. Rabsch W, Voigt W, Reissbrodt R, Tsolis RM, Baumler AJ. Salmonella typhimurium IroN and FepA proteins mediate uptake of enterobactin but differ in their specificity for other siderophores. J Bacteriol. 1999; 181:3610–3612. [PubMed: 10348879]
7. Tsolis RM, Baumler AJ, Heffron F, Stojiljkovic I. Contribution of TonB- and Feo-mediated iron uptake to growth of Salmonella typhimurium in the mouse. Infect Immun. 1996; 64:4549–4556. [PubMed: 8890205]
8. Zhou D, Hardt WD, Galan JE. Salmonella typhimurium encodes a putative iron transport system within the centisome 63 pathogenicity island. Infect Immun. 1999; 67:1974–1981. [PubMed: 10085045]
9. Boyer E, Bergevin I, Malo D, Gros P, Cellier MF. Acquisition of Mn(II) in addition to Fe(II) is required for full virulence of Salmonella enterica serovar Typhimurium. Infect Immun. 2002; 70:6032–6042. [PubMed: 12379679]
10. Janakiraman A, Slauch JM. The putative iron transport system SitABCD encoded on SPI1 is required for full virulence of Salmonella typhimurium. Mol Microbiol. 2000; 35:1146–1155. [PubMed: 10712695]
11. Schaible UE, Kaufmann SH. Iron and microbial infection. Nat Rev Microbiol. 2004; 2:946–953. [PubMed: 15550940]
12. Nairz M, Schroll A, Sonnweber T, Weiss G. The struggle for iron - a metal at the host-pathogen interface. Cell Microbiol. 2010; 12:1691–1702. [PubMed: 20964797]
13. Cairo G, Recalcati S, Mantovani A, Locati M. Iron trafficking and metabolism in macrophages: contribution to the polarized phenotype. Trends Immunol. 2011; 32:241–247. [PubMed: 21514223]

Author Manuscript Author Manuscript Author Manuscript Author Manuscript

14. Drakesmith H, Prentice AM. Hepcidin and the iron-infection axis. Science. 2012; 338:768–772. [PubMed: 23139325]
15. Weiss G. Iron and immunity: a double-edged sword. Eur J Clin Invest. 2002; 32(Suppl 1):70–78. [PubMed: 11886435]
16. Weinberg ED. Iron availability and infection. Biochim Biophys Acta. 2009; 1790:600–605. [PubMed: 18675317]
17. Andrews NC, Schmidt PJ. Iron homeostasis. Annu Rev Physiol. 2007; 69:69–85. [PubMed: 17014365]
18. Ganz T. Macrophages and Systemic Iron Homeostasis. J Innate Immun. 2014; 4:446–453. [PubMed: 22441209]
19. Hentze MW, Muckenthaler MU, Andrews NC. Balancing acts: molecular control of mammalian iron metabolism. Cell. 2004; 117:285–297. [PubMed: 15109490]
20. Scaccabarozzi A, Arosio P, Weiss G, Valenti L, Dongiovanni P, Fracanzani AL, Mattioli M, et al. Relationship between TNF-alpha and iron metabolism in differentiating human monocytic THP-1 cells. Br J Haematol. 2000; 110:978–984. [PubMed: 11054092]
21. Ludwiczek S, Aigner E, Theurl I, Weiss G. Cytokine-mediated regulation of iron transport in human monocytic cells. Blood. 2003; 101:4148–4154. [PubMed: 12522003]
22. Weiss G. Modification of iron regulation by the inflammatory response. Best Pract Res Clin Haematol. 2005; 18:183–201. [PubMed: 15737884]
23. Peyssonnaux C, Zinkernagel AS, Datta V, Lauth X, Johnson RS, Nizet V. TLR-4 dependent hepcidin expression by myeloid cells in response to bacterial pathogens. Blood. 2006; 107:3727–3732. [PubMed: 16391018]
24. Weiss G, Goodnough LT. Anemia of chronic disease. N Engl J Med. 2005; 352:1011–1023. [PubMed: 15758012]
25. Nemeth E, Tuttle MS, Powelson J, Vaughn MB, Donovan A, Ward DM, Ganz T, Kaplan J. Hepcidin regulates cellular iron efflux by binding to ferroportin and inducing its internalization. Science. 2004; 306:2090–2093. [PubMed: 15514116]
26. Weinberg ED. Patho-ecological implications of microbial acquisition of host iron. Reviews in Medical Microbiology. 1998; 9:171–178.
27. Theurl I, Aigner E, Theurl M, Nairz M, Seifert M, Schroll A, Sonnweber T, et al. Regulation of iron homeostasis in anemia of chronic disease and iron deficiency anemia: diagnostic and therapeutic implications. Blood. 2009; 113:5277–5286. [PubMed: 19293425]
28. Nairz M, Fritsche G, Crouch ML, Barton HC, Fang FC, Weiss G. Slc11a1 limits intracellular growth of Salmonella enterica sv. Typhimurium by promoting macrophage immune effector functions and impairing bacterial iron acquisition. Cell Microbiol. 2009; 11:1365–1381. [PubMed: 19500110]
29. Kim DK, Jeong JH, Lee JM, Kim KS, Park SH, Kim YD, Koh M, et al. Inverse agonist of estrogen-related receptor gamma controls Salmonella typhimurium infection by modulating host iron homeostasis. Nat Med. 2014; 20:419–424. [PubMed: 24658075]
30. Nairz M, Schleicher U, Schroll A, Sonnweber T, Theurl I, Ludwiczek S, Talasz H, et al. Nitric oxide-mediated regulation of ferroportin-1 controls macrophage iron homeostasis and immune function in Salmonella infection. J Exp Med. 2013; 210:855–873. [PubMed: 23630227]
31. Flo TH, Smith KD, Sato S, Rodriguez DJ, Holmes MA, Strong RK, Akira S, Aderem A. Lipocalin 2 mediates an innate immune response to bacterial infection by sequestrating iron. Nature. 2004; 432:917–921. [PubMed: 15531878]
32. Berger T, Togawa A, Duncan GS, Elia AJ, You-Ten A, Wakeham A, Fong HE, et al. Lipocalin 2-deficient mice exhibit increased sensitivity to Escherichia coli infection but not to ischemia-reperfusion injury. Proc Natl Acad Sci U S A. 2006; 103:1834–1839. [PubMed: 16446425]
33. Deriu E, Liu JZ, Pezeshki M, Edwards RA, Ochoa RJ, Contreras H, Libby SJ, et al. Probiotic bacteria reduce salmonella typhimurium intestinal colonization by competing for iron. Cell Host Microbe. 2013; 14:26–37. [PubMed: 23870311]
34. Guglani L, Gopal R, Rangel-Moreno J, Junecko BF, Lin Y, Berger T, Mak TW, et al. Lipocalin 2 regulates inflammation during pulmonary mycobacterial infections. PLoS One. 2012; 7:e50052. [PubMed: 23185529]

Author Manuscript Author Manuscript Author Manuscript Author Manuscript

35. Saiga H, Nishimura J, Kuwata H, Okuyama M, Matsumoto S, Sato S, Matsumoto M, et al. Lipocalin 2-dependent inhibition of mycobacterial growth in alveolar epithelium. J Immunol. 2008; 181:8521–8527. [PubMed: 19050270]
36. Holmes MA, Paulsene W, Jide X, Ratledge C, Strong RK. Siderocalin (Lcn 2) also binds carboxymycobactins, potentially defending against mycobacterial infections through iron sequestration. Structure. 2005; 13:29–41. [PubMed: 15642259]
37. Devireddy LR, Gazin C, Zhu X, Green MR. A cell-surface receptor for lipocalin 24p3 selectively mediates apoptosis and iron uptake. Cell. 2005; 123:1293–1305. [PubMed: 16377569]
38. Devireddy LR, Hart DO, Goetz DH, Green MR. A mammalian siderophore synthesized by an enzyme with a bacterial homolog involved in enterobactin production. Cell. 2010; 141:1006–1017. [PubMed: 20550936]
39. Bao G, Clifton M, Hoette TM, Mori K, Deng SX, Qiu A, Viltard M, et al. Iron traffics in circulation bound to a siderocalin (Ngal)-catechol complex. Nat Chem Biol. 2010; 6:602–609. [PubMed: 20581821]
40. Liu Z, Reba S, Chen WD, Porwal SK, Boom WH, Petersen RB, Rojas R, et al. Regulation of mammalian siderophore 2,5-DHBA in the innate immune response to infection. J Exp Med. 2014; 211:1197–1213. [PubMed: 24863067]
41. Nelson AL, Ratner AJ, Barasch J, Weiser JN. Interleukin-8 secretion in response to aferric enterobactin is potentiated by siderocalin. Infect Immun. 2007; 75:3160–3168. [PubMed: 17420239]
42. Schroll A, Eller K, Feistritzer C, Nairz M, Sonnweber T, Moser PA, Rosenkranz AR, et al. Lipocalin-2 ameliorates granulocyte functionality. Eur J Immunol. 2012; 42:3346–3357. [PubMed: 22965758]
43. Liu Z, Petersen R, Devireddy L. Impaired neutrophil function in 24p3 null mice contributes to enhanced susceptibility to bacterial infections. J Immunol. 2013; 190:4692–4706. [PubMed: 23543755]
44. Raffatellu M, George MD, Akiyama Y, Hornsby MJ, Nuccio SP, Paixao TA, Butler BP, et al. Lipocalin-2 resistance confers an advantage to Salmonella enterica serotype Typhimurium for growth and survival in the inflamed intestine. Cell Host Microbe. 2009; 5:476–486. [PubMed: 19454351]
45. Cassat JE, Skaar EP. Iron in infection and immunity. Cell Host Microbe. 2013; 13:509–519. [PubMed: 23684303]
46. Chakraborty S, Kaur S, Guha S, Batra SK. The multifaceted roles of neutrophil gelatinase associated lipocalin (NGAL) in inflammation and cancer. Biochim Biophys Acta. 2012; 1826:129–169. [PubMed: 22513004]
47. Borregaard N, Cowland JB. Neutrophil gelatinase-associated lipocalin, a siderophore-binding eukaryotic protein. Biometals. 2006; 19:211–215. [PubMed: 16718606]
48. Bellmann-Weiler R, Schroll A, Engl S, Nairz M, Talasz H, Seifert M, Weiss G. Neutrophil gelatinase-associated lipocalin and interleukin-10 regulate intramacrophage Chlamydia pneumoniae replication by modulating intracellular iron homeostasis. Immunobiology. 2013; 218:969–978. [PubMed: 23317919]
49. Warszawska JM, Gawish R, Sharif O, Sigel S, Doninger B, Lakovits K, Mesteri I, et al. Lipocalin 2 deactivates macrophages and worsens pneumococcal pneumonia outcomes. J Clin Invest. 2013; 123:3363–3372. [PubMed: 23863624]
50. Taub N, Nairz M, Hilber D, Hess MW, Weiss G, Huber LA. The late endosomal adaptor p14 is a macrophage host defense factor against Salmonella Typhimurium infection. J Cell Sci. 2012; 125:2698–2708. [PubMed: 22427693]
51. Srinivasan G, Aitken JD, Zhang B, Carvalho FA, Chassaing B, Shashidharamurthy R, Borregaard N, et al. Lipocalin 2 deficiency dysregulates iron homeostasis and exacerbates endotoxin-induced sepsis. J Immunol. 2012; 189:1911–1919. [PubMed: 22786765]
52. Nairz M, Theurl I, Schroll A, Theurl M, Fritsche G, Lindner E, Seifert M, et al. Absence of functional Hfe protects mice from invasive Salmonella enterica serovar Typhimurium infection via induction of lipocalin-2. Blood. 2009; 114:3642–3651. [PubMed: 19700664]

Author Manuscript Author Manuscript Author Manuscript Author Manuscript

53. Bellmann-Weiler R, Martinz V, Kurz K, Engl S, Feistritzer C, Fuchs D, Rupp J, et al. Divergent modulation of Chlamydia pneumoniae infection cycle in human monocytic and endothelial cells by iron, tryptophan availability and interferon gamma. Immunobiology. 2010; 215:842–848. [PubMed: 20646782]

54. Theurl M, Theurl I, Hochegger K, Obrist P, Subramaniam N, van Rooijen N, Schuemann K, Weiss G. Kupffer cells modulate iron homeostasis in mice via regulation of hepcidin expression. J Mol Med. 2008; 86:825–835. [PubMed: 18521557]

55. Ludwiczek S, Theurl I, Artner-Dworzak E, Chorney M, Weiss G. Duodenal HFE expression and hepcidin levels determine body iron homeostasis: modulation by genetic diversity and dietary iron availability. J Mol Med. 2004; 82:373–382. [PubMed: 15173932]

56. Schimanski LM, Drakesmith H, Merryweather-Clarke AT, Viprakasit V, Edwards JP, Sweetland E, Bastin JM, et al. In vitro functional analysis of human ferroportin (FPN) and hemochromatosis-associated FPN mutations. Blood. 2005; 105:4096–4102. [PubMed: 15692071]

57. Kuhn R, Lohler J, Rennick D, Rajewsky K, Muller W. Interleukin-10-deficient mice develop chronic enterocolitis. Cell. 1993; 75:263–274. [PubMed: 8402911]

58. Theurl I, Theurl M, Seifert M, Mair S, Nairz M, Rumpold H, Zoller H, et al. Autocrine formation of hepcidin induces iron retention in human monocytes. Blood. 2008; 111:2392–2399. [PubMed: 18073346]

59. Drakesmith H, Schimanski LM, Ormerod E, Merryweather-Clarke AT, Viprakasit V, Edwards JP, Sweetland E, et al. Resistance to hepcidin is conferred by hemochromatosis-associated mutations of ferroportin. Blood. 2005; 106:1092–1097. [PubMed: 15831700]

60. Mayr R, Griffiths WJ, Hermann M, McFarlane I, Halsall DJ, Finkenstedt A, Douds A, et al. Identification of mutations in SLC40A1 that affect ferroportin function and phenotype of human ferroportin iron overload. Gastroenterology. 2011; 140:2056–2063. 2063 e2051. [PubMed: 21396368]

Abbreviations

ANOVA	analysis of variance
CytD	cytochalasin D
DFX	deferasirox
Fpn1	ferroportin-1
Ft	ferritin
Hamp1	hepcidin antimicrobial peptide-1
Lcn2	lipocalin-2
LcnR	Lcn2 receptor
MPS	mononuclear phagocyte system
qRT-PCR	quantitative reverse-transcription polymerase chain reaction

Author Manuscript Author Manuscript Author Manuscript Author Manuscript

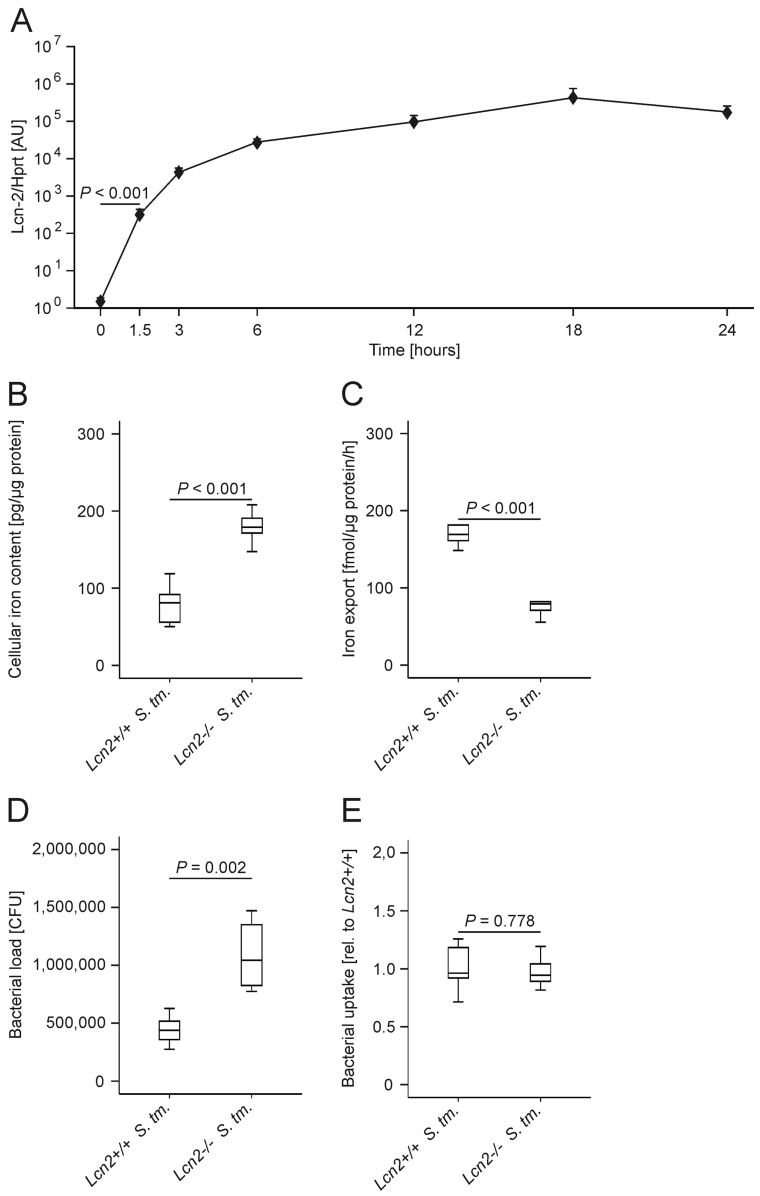

Figure 1. Altered iron homeostasis in *Lcn2*$^{-/-}$ peritoneal macrophagesupon *Salmonella* Typhimurium infection

(A) C57BL/6 wt thioglycolate-elicited peritoneal macrophages were treated with PBS (0 h) or infected with *Salmonella* Typhimurium at a multiplicity of 10 for 1.5 to 24 h. Lcn2 expression was determined by qRT-PCR, data were normalized for mRNA levels of Hprt. Statistically significant differences were calculated by ANOVA using Bonferroni correction following log-transformation ($P < 0.001$ for each of the comparisons relative to PBS treatment). Values are depicted on a semi-logarithmic scale as means ± S.E.M ($n = 4$ independent experiments). (B) *Wt* and *Lcn2*$^{-/-}$ peritoneal macrophages were infected with *Salmonella* Typhimurium (*S.* Tm.) for 24 h. The iron content was determined by atomic absorption spectrometry. Values are depicted as lower quartile, median and upper quartile (boxes) with minimum and maximum ranges and statistical significant differences as

Author Manuscript Author Manuscript Author Manuscript Author Manuscript

determined by *t* test are indicated (n = 4-5 individual mice per group). One representative experiment out of 2 independent experiments is shown. (C) ^{59}Fe transport studies were used to determine macrophage iron release following infection with *Salmonella* Typhimurium (*S.* Tm.) . Values are depicted as lower quartile, median and upper quartile (boxes) with minimum and maximum ranges and statistical significant differences as determined by *t* test are indicated (n = 6 independent experiments). (D) In parallel, the intracellular bacterial load was determined by plating serial dilutions of peritoneal macrophages lysates. Values are depicted as lower quartile, median and upper quartile (boxes) with minimum and maximum ranges and statistical significant differences as determined by *t* test are indicated. (n = 6 independent experiments). (E) *Wt* and *Lcn2*$^{-/-}$ peritoneal macrophages were infected with *Salmonella* Typhimurium (*S.* Tm.) for 30 min. Thereafter, bacterial uptake was determined by plating serial dilutions of peritoneal macrophages lysates. Values are depicted as lower quartile, median and upper quartile (boxes) with minimum and maximum ranges and statistical significant differences as determined by *t* test are indicated. (n = 6 independent experiments).

Author Manuscript Author Manuscript Author Manuscript Author Manuscript

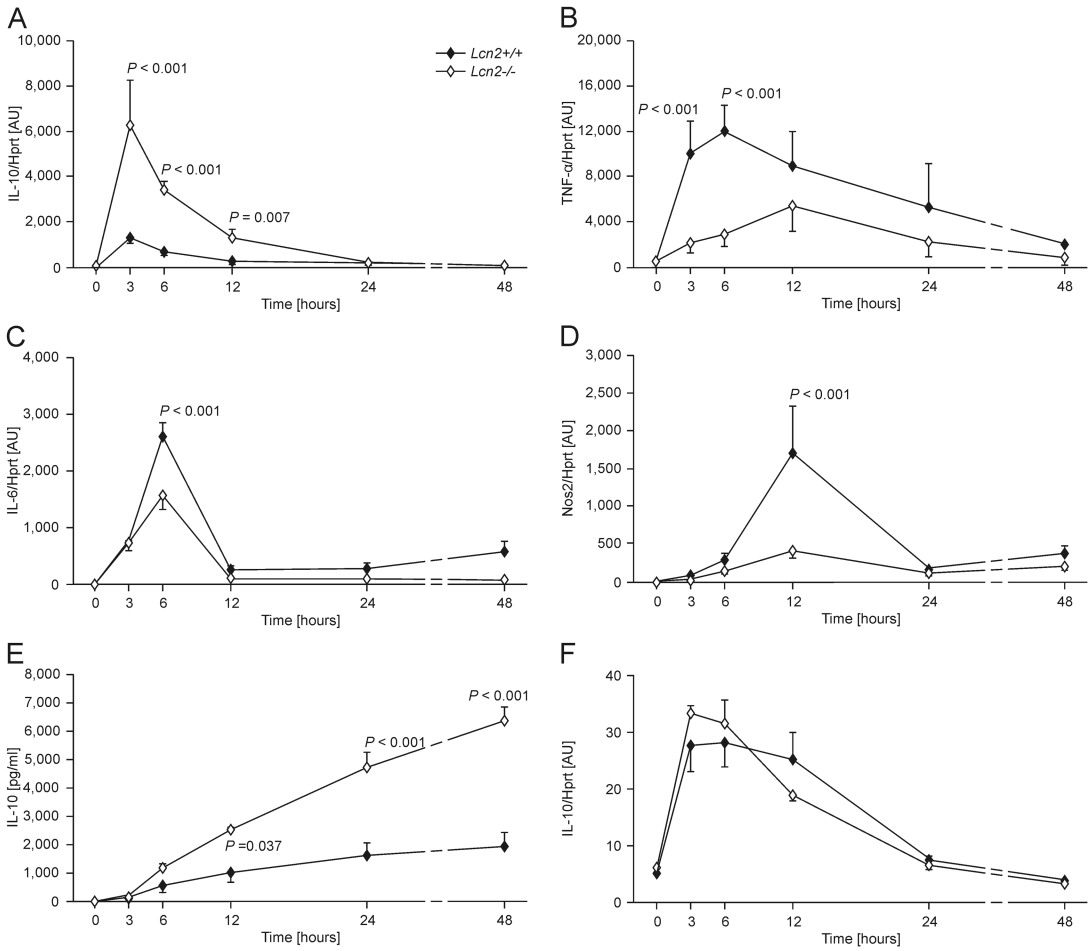

Figure 2. Time-dependent differences in immune genes expression between *wt* and *Lcn2*$^{-/-}$ peritoneal macrophages

Wt (closed symbols) and *Lcn2*$^{-/-}$ peritoneal macrophages (open symbols) were treated with PBS (Ctrl.) or infected with *Salmonella* Typhimurium (*S.* Tm.) for 3 to 48 h. IL-10 (A), TNF-α (B), IL-6 (C) and Nos2 (D) expression was determined by qRT-PCR, and data were normalized for mRNA levels of Hprt and compared by ANOVA using Bonferroni's correction for multiple tests. Values are depicted as means ± S.E.M and statistically significant differences between cells of the two genotypes are indicated (n = 4-12 individual values from 4 independent experiments). (E) IL-10 concentrations in cell culture supernatants were determined by a specific ELISA. IL-10 concentrations in PBS-treated cells were below the detection limit of the ELISA kit used and are depicted as 0. Data were compared by ANOVA using Bonferroni's correction for multiple tests. Values are depicted as means ± S.E.M and statistically significant differences between cells of the two genotypes are indicated (n = 4 individual values from 4 independent experiments). (F) In parallel, *Lcn2*$^{+/+}$ and *Lcn2*$^{-/-}$ peritoneal macrophages were treated with PBS (Ctrl.) or with the same number of heat-inactivated *Salmonella* Typhimurium (*S.* Tm.) for 3 to 48 h. IL-10 mRNA expression was determined by qRT-PCR, and data compared by ANOVA using Bonferroni's correction for multiple tests. Values are depicted as means ± S.E.M and statistically significant differences between cells of the two genotypes are indicated (n = 4-12 individual

values from 4 independent experiments). Note that the x-axis is non-linear between the 24 and 48 h time-points for the sake of better illustration.

Author Manuscript Author Manuscript Author Manuscript Author Manuscript

Author Manuscript Author Manuscript Author Manuscript Author Manuscript

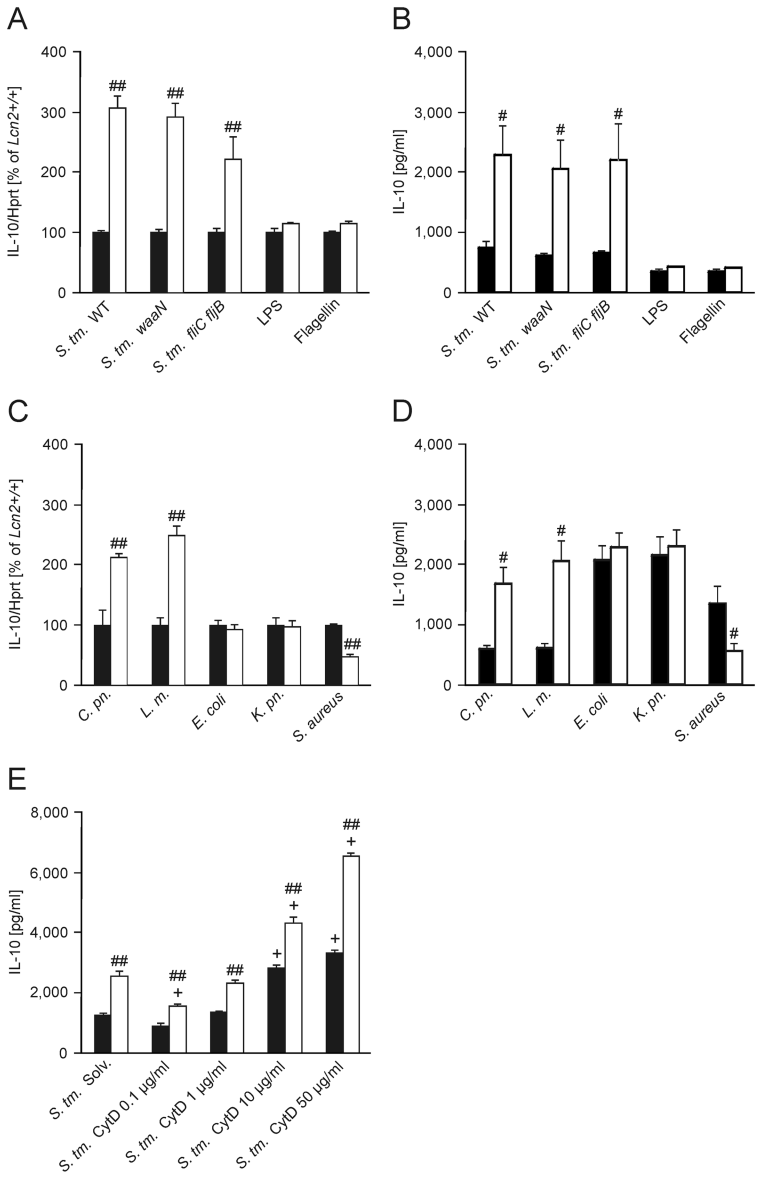

Figure 3. Lcn2 affects IL-10 mRNA expression in response to intracellular pathogens

(A) *Wt* (closed bars) and *Lcn2*$^{-/-}$ peritoneal macrophages (open bars) were infected with *Salmonella* Typhimurium (*S.* Tm.) *wt* or isogenic mutants with modified LPS (*waaN*) or lacking flagellin (*fliC fljB*) at a MOI of 10:1 for 3 h. In parallel, *wt* and *Lcn2*$^{-/-}$ peritoneal macrophages were treated with 100 ng/ml LPS or flagellin isolated from *Salmonella* Typhimurium (n = 6 individual values from 4 independent experiments). IL-10 mRNA expression was determined by qRT-PCR and normalized for mRNA levels of Hprt. Results are reported relative to expression in *wt* peritoneal macrophages. Bars show means + S.E.M. from 6 independent experiments. *P* values were compared by independent sample *t* test. ## *P* value < 0.01 for the comparison of the two *Lcn2* genotypes. (B) IL-10 secretion was assessed by measuring cytokine concentrations in culture supernatants of cells infected/stimulated for 6 h by ELISA. Data were compared as in A. Bars show means + S.E.M. from

Author Manuscript Author Manuscript Author Manuscript Author Manuscript

4-5 experiments. # *P* value < 0.05 for the comparison of the two *Lcn2* genotypes. (C) *Wt* and *Lcn2*$^{-/-}$ peritoneal macrophages were infected for 3 h at a MOI of 10 with *Chlamydia pneumoniae* (*C. pn.*), *Listeria monocytogenes* (*L. m.*), *Escherichia coli* (*E. coli*), *Klebsiella pneumoniae* (*K. pn.*) or *Staphylococcus aureus* (*S. aureus*). IL-10 mRNA expression relative to Hprt levels was determined and reported as in A. Bars show means + S.E.M. from 6 independent experiments. (D) IL-10 secretion was assessed by measuring cytokine concentrations in culture supernatants of cells infected for 6 h. Data were compared as in A (n = 4 independent experiments). # *P* value < 0.05 for the comparison of the two *Lcn2* genotypes. Bars show means + S.E.M. from 4 independent experiments. (E) *Wt* and *Lcn2*$^{-/-}$ BMDM were preincubated with increasing concentrations of cytochalasin D (CytD) as indicated for 1 h and subsequently infected for 12 h before supernatants were harvested for IL-10 measurement (n = 3 independent experiments). Bars show means + S.E.M. from 3 independent experiments. ## *P* value < 0.01 for the comparison of the two *Lcn2* genotypes. + *P* value < 0.01 for the comparison to solvent-treated cells of the respective genotype.

Author Manuscript Author Manuscript Author Manuscript Author Manuscript

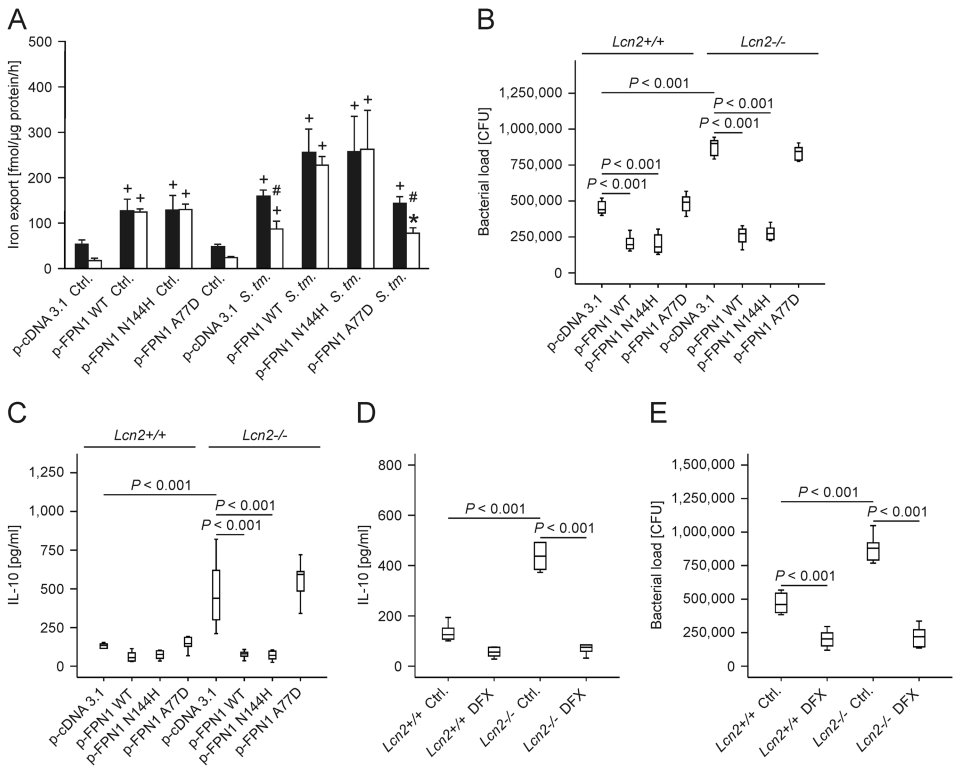

Figure 4. Forced expression of FPN1 or iron chelation by DFX rescues the phenotype of *Lcn2*$^{-/-}$ peritoneal macrophages

(A) *Wt* (closed bars) and *Lcn2*$^{-/-}$ peritoneal macrophages (open bars) were transiently transfected with empty plasmid (p-cDNA3.1) or expression constructs containing the indicated human FPN1 variants. ^{59}Fe transport studies were used to determine macrophage iron release following treatment with diluent (Ctrl.) or infection with *wt Salmonella* Typhimurium (*S.* Tm.). Values are depicted as means ± S.E.M. and statistically significant differences as calculated by ANOVA are indicated (n = 4 independent experiments). # P value < 0.01 for the comparison of *wt* and *Lcn2*$^{-/-}$ peritoneal macrophages. + P value < 0.001 as compared to the control of the respective genotype. * P value = 0.003 as compared to the control of the respective genotype. (B, C) The bacterial load (B) in macrophages was quantified by plating of cell lysates on LB agar and the accumulation of IL-10 (C) in cell culture supernatants was measured by an ELISA kit. Values are depicted as as means ± S.E.M. lower quartile, median and upper quartile (boxes) with minimum and maximum ranges and statistically significant differences are indicated (n = 6 independent experiments). (D, E) The bacterial load and IL-10 production was quantified following treatment with 50 µM DFX (n = 6 independent experiments). Bars show lower quartile, median and upper quartile (boxes) with minimum and maximum ranges and statistical significant differences as determined by ANOVA are indicated.

Author Manuscript Author Manuscript Author Manuscript Author Manuscript

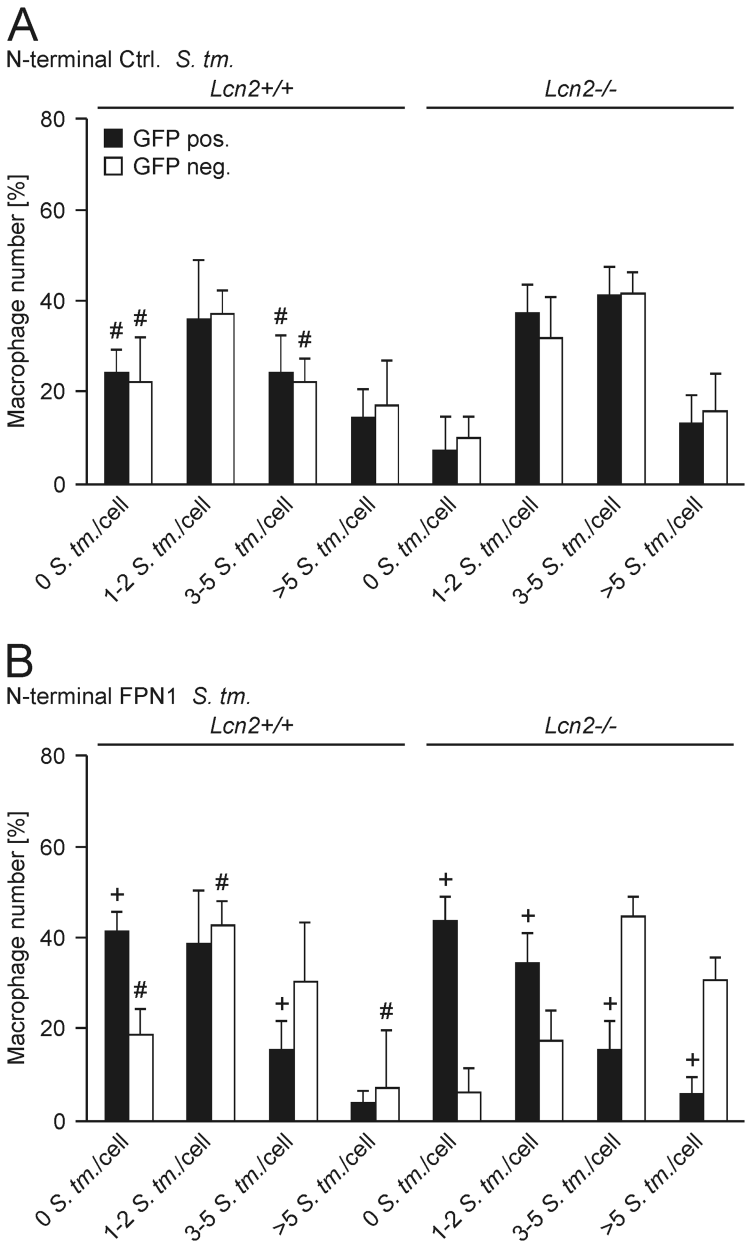

Author Manuscript Author Manuscript Author Manuscript Author Manuscript

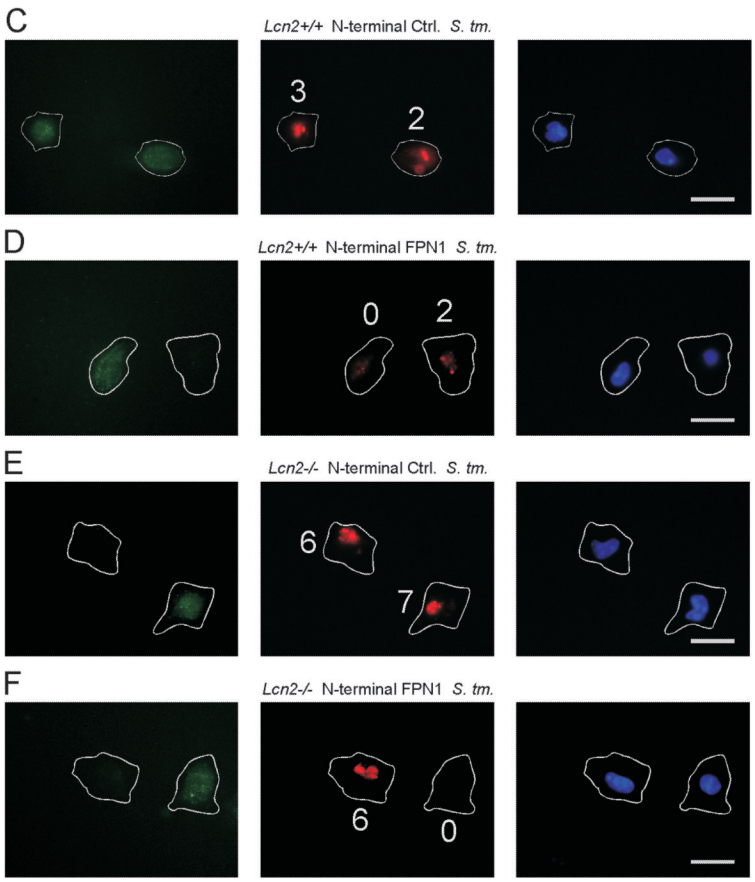

Figure 5. Forced expression of FPN1 reduces *Salmonella* numbers in *Lcn2*$^{-/-}$ peritoneal macrophages

(A-F) *Wt* (left-hand side in A and B) and *Lcn2*$^{-/-}$ (right-hand side in A and B) peritoneal macrophages were transfected with empty plasmid encoding only for EmGFP (A) or the N-terminal EmGFP-FPN1 construct (B). The latter allowed us to identify FPN1 over-expressing cells through the detection of EmGFP. Subsequently, cells were infected with *S.* Typhimurium for 16 h. The number of intracellular bacteria was determined by immunofluorescence. (A, B) The number of intracellular bacteria is depicted as a function of GFP expression. For evaluation, peritoneal macrophages were grouped into 4 categories containing 0, 1-2, 3-5 or more than 5 bacteria per macrophage. Bars show means + S.E.M. from from 4 independent experiments. Data were compared by ANOVA followed by Bonferroni's correction (n = 4 independent experiments). #, $P < 0.05$ for the comparison of *wt* and *Lcn2*$^{-/-}$ peritoneal macrophages; +, $P < 0.05$ for the comparison between GFP^{+} (closed bars) and GFP^{-} peritoneal macrophages (open bars). (C-F) Representative images acquired at 1000× magnification are depicted. Left panel: GFP in green. Middle panel: CSA1/*S.* Typhimurium in red. Right panel: DAPI/nucleus in blue. The cell membrane and the number of intracellular bacteria are indicated. Scale bars: 20 μm. (C, D) *Wt* peritoneal macrophages were transiently transfected with empty EmGFP N-terminal plasmid (C) or a FPN1-EmGFP N-terminal construct (D), respectively. (E, F) *Lcn2*$^{-/-}$ peritoneal macrophages were transiently transfected with empty EmGFP N-terminal plasmid (E) or a FPN1-EmGFP N-terminal construct (F), respectively.

Author Manuscript Author Manuscript Author Manuscript Author Manuscript

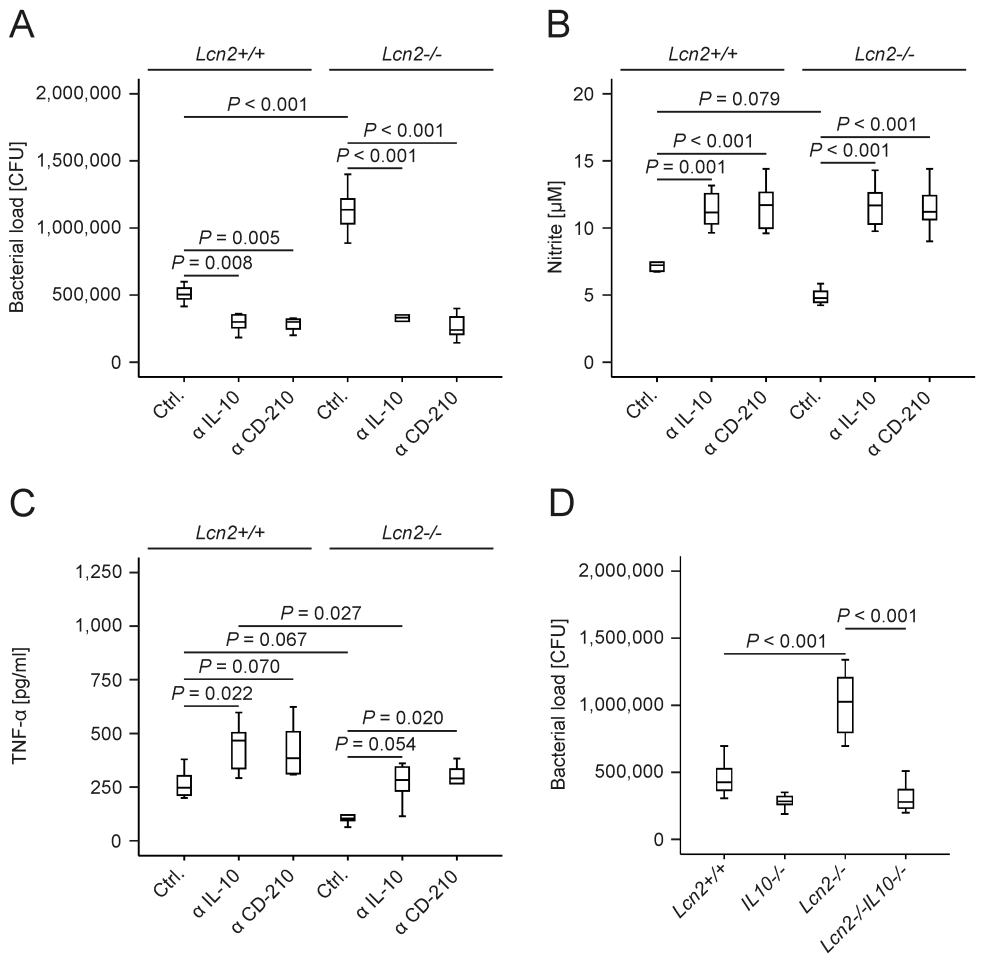

Figure 6. Blocking or absence of IL-10 rescues the phenotype of *Lcn2*$^{-/-}$ macrophages

(A) The bacterial load in *wt* and *Lcn2*$^{-/-}$ peritoneal macrophages treated with a neutralizing IL-10 antibody, a blocking CD-210 antibody or the respective isotype control was quantified by plating of cell lysates on LB agar. Values were compared by ANOVA followed by Bonferroni's correction and are depicted as means ± S.E.M., lower quartile, median and upper quartile (boxes) with minimum and maximum ranges and statistically significant differences as indicated (*n* = 6 independent experiments). (B, C) Nitrite and TNF-α concentrations in culture supernatants were determined by the Griess reaction and a specific ELISA, respectively. Values were compared by ANOVA followed by Bonferroni's correction and are depicted as means ± S.E.M., lower quartile, median and upper quartile (boxes) with minimum and maximum ranges and statistically significant differences as indicated (*n* = 6 independent experiments). (D) Peritoneal macrophages from *wt*, *Lcn2*$^{-/-}$, *IL-10*$^{-/-}$ and *Lcn2*$^{-/-}$ *IL-10*$^{-/-}$ mice were infected with *Salmonella* Typhimurium (*S.* Tm.). The bacterial load was quantified after 24 h (*n* = 6-12 independent experiments). Values were compared by ANOVA followed by Bonferroni's correction and are depicted as means ± S.E.M., lower quartile, median and upper quartile (boxes) with minimum and maximum ranges and statistically significant differences as indicated.

Author Manuscript Author Manuscript Author Manuscript Author Manuscript

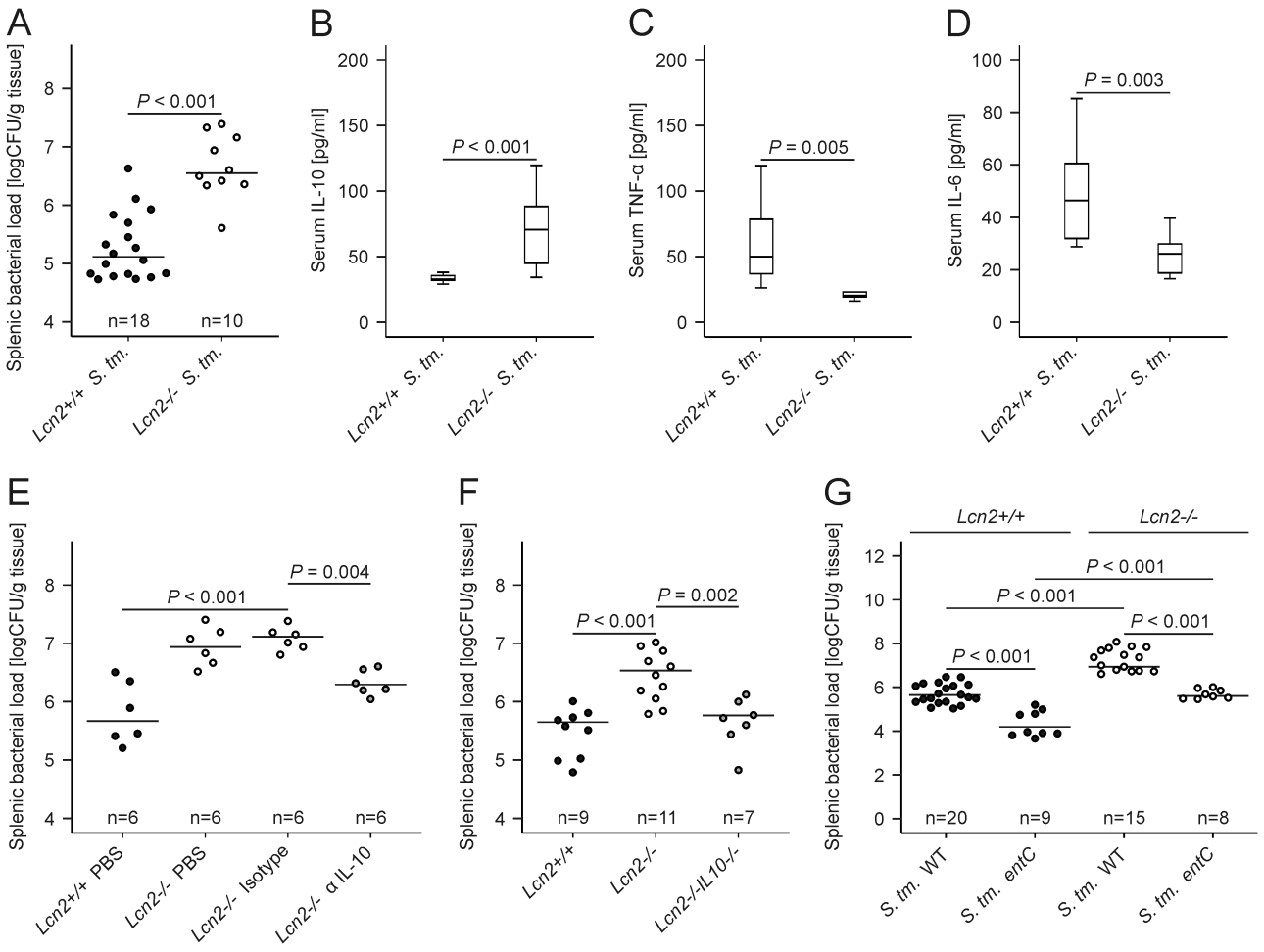

Figure 7. IL-10 neutralization or deletion restores bacterial killing in *Lcn2*$^{-/-}$ mice

(A-D) *Wt* and *Lcn2*$^{-/-}$ mice were infected with 500 CFU *wt Salmonella* Typhimurium (*S.* Tm.) for 72 h. The bacterial load in spleen was determined by plating serial dilutions of tissue lysates (A). Serum concentrations of IL-10 (B), TNF-α (C) and IL-6 (D) of *Salmonella* Typhimurium-infected *wt* and *Lcn2*$^{-/-}$ mice were determined by a specific ELISA after 72 h. (A) Each dot shows an individual mouse, bars indicate means (B-D) Results were compared by *t* test and are depicted as lower quartile, median and upper quartile (boxes) with minimum and maximum ranges and statistical significance between mice of the two genotypes as indicated (*n* = 10-18 individual mice per group). (E) *Wt* and *Lcn2*$^{-/-}$ mice were infected with *wt Salmonella* Typhimurium (*S.* Tm.) for 72 h. *Lcn2*$^{-/-}$ mice were enrolled in 1 of 3 treatment groups receiving either solvent (PBS), a control monoclonal IgG antibody (isotype) or a neutralizing monoclonal IL-10 antibody (α IL-10). *Wt* mice were treated with solvent and the bacterial load in spleen was determined by plating serial dilutions of tissue lysates. Each dot shows an individual mouse, bars indicate means. Values were log-transformed and compared by ANOVA using Bonferroni correction (*n* as indicated). (F) *Wt* (closed circles), *Lcn2*$^{-/-}$ (open circles) and *Lcn2*$^{-/-}$ *IL-10*$^{-/-}$ mice (grey circles) were infected with *wt Salmonella* Typhimurium (*S.* Tm.) for 72 h. The bacterial load in spleen was determined by plating serial dilutions of tissue lysates. Each dot shows an

Author Manuscript Author Manuscript Author Manuscript Author Manuscript

individual mouse, bars indicate means. Values were log-transformed and compared by ANOVA using Bonferroni correction (*n* as indicated). (G) *Wt* and *Lcn2*$^{-/-}$ mice were infected with 500 CFU *wt Salmonella* Typhimurium (*S.* Tm.) or the siderophore-deficient *entC* mutant for 72 h. The bacterial load in spleen was determined by plating serial dilutions of tissue lysates. Each dot shows an individual mouse, bars indicate means. Values were log-transformed and compared by ANOVA using Bonferroni correction (*n* as indicated).

Author Manuscript

Author Manuscript

Author Manuscript

Author Manuscript

Table 1

Relative mRNA expression of splenic immune genes 72 h after onset of *Salmonella* Typhimurium (*S.* Tm.) infection in *wt* and congenic *Lcn2*$^{-/-}$ mice

Male C57BL/6N and *Lcn2*$^{-/-}$ littermates were i.p. infected with 500 CFU *Salmonella* Typhimurium (*S.* Tm.) for 72 h, while control mice received an i.p. injection of 200 µl PBS as diluent. Quantitative reverse-transcription polymerase chain reaction (qRT-PCR) was used to analyze mRNA levels of immune response genes in the spleen. Data are normalized for mRNA levels of the housekeeping gene Hprt and are shown as arbitrary units (AU). Results were compared by Kruskall-Wallis test and are listed as means ± S.E.M. (n = 10-18 individual mice per group).

Stimulation Gene name	*Control wt (Lcn2*$^{+/+}$*)*	*Control Lcn2*$^{-/-}$	*S.* Tm. *wt (Lcn2*$^{+/+}$*)*	*S.* Tm. *Lcn2*$^{-/-}$
IL-10 [AU]	0.84 ± 0.73	1.13 ± 1.19	4.16 ± 3.52 [a]	40.63 ± 8.77 [b,c]
Nos2 [AU]	0.06 ± 0.03	0.08 ± 0.06	19.06 ± 7.03 [a]	6.27 ± 2.69 [b,c]
p47-phox [AU]	5.33 ± 1.91	4.82 ± 2.71	23.45 ± 6.53 [a]	25.51 ± 11.40 [b]
TNF-α [AU]	3.69 ± 1.82	4.14 ± 3.08	164.30 ± 27.90 [a]	40.47 ± 22.49 [b,c]
IL-1β [AU]	13.02 ± 6.53	18.93 ± 9.46	180.20 ± 69.45 [a]	139.99 ± 92.89 [b]
IL-4 [AU]	0.42 ± 1.00	0.65 ± 0.57	4.95 ± 7.03 [a]	4.27 ± 1.71 [b]
IL-6 [AU]	0.35 ± 0.12	0.39 ± 0.19	11.70 ± 5.37 [a]	6.82 ± 6.10 [b,c]
IL-17A [AU]	0.01 ± 0.00	0.02 ± 0.01	9.06 ± 11.10 [a]	8.92 ± 4.38 [b]
IFN-γ [AU]	2.06 ± 2.86	0.88 ± 1.21 [a]	39.74 ± 45.13 [a]	19.61 ± 33.67 [b]

[a] $P < 0.05$ as compared to uninfected (Ctrl.) *wt (Lcn2*$^{+/+}$*)* mice.

[b] $P < 0.05$ as compared to uninfected (Ctrl.) *Lcn2*$^{-/-}$ mice.

[c] $P < 0.05$ for comparison of *S.* Tm.-infected *wt (Lcn2*$^{+/+}$*)* and *S.* Tm.-infected *Lcn2*$^{-/-}$ mice.

AU… arbitrary units of target gene expression relative to the level of the housekeeping gene Hprt.